International Journal of Disaster Risk Reduction 132 (2026) 105965

Contents lists available at ScienceDirect

International Journal of Disaster Risk Reduction

journal homepage: www.elsevier.com/locate/ijdrr

An impact risk assessment methodology for the evaluation of the economic, social and operational resilience of critical infrastructures

Antonio Di Pietro [a],*, Alberto Tofani [a], Clemente Fuggini [b], Celina Solari [b], Gabriele Oliva [c]

[a] ENEA, Italian National Agency for New Technologies, Energy and Sustainable Economic Development, Rome, Italy
[b] RINA Consulting S.p.A., Genoa, Italy
[c] Campus Bio-Medico University of Rome, Italy

ARTICLE INFO

Keywords:
Critical infrastructure
Cascading risk
Resilience
Dependency graph
Social impact
Preparedness

ABSTRACT

Critical infrastructures are increasingly exposed to multi-hazard events and cascading failures arising from their interdependencies. This paper refines and extends the MARIS methodology, originally developed for the analysis of dependency risks, by integrating recovery dynamics and probabilistic modeling of disruption parameters. The enhanced framework supports a comprehensive assessment of cascading effects and resilience across social, economic, and operational dimensions. Its application to the city of Camerino (Italy) illustrates the practicality of the approach in a real urban setting. Results highlight differing resilience levels along dependency chains and offer insights for preparedness and mitigation planning. Overall, the study confirms the potential of MARIS as a transparent and adaptable decision-support tool for resilience planning under multi-hazard conditions.

1. Introduction

Cascading failures represent a critical threat in urban systems, where the disruption of a single component can propagate across multiple interdependent Critical Infrastructures (CIs). The tight coupling among power grids, transport networks, communication systems, and healthcare services means that localized failures may evolve into systemic crises. Notable examples include the Valencia flood of October 2024, where extreme rainfall triggered widespread disruptions across mobility, energy, and emergency services [1], and Hurricane Sandy (2012), which caused prolonged power outages with cascading impacts on transportation, healthcare, and telecommunications in New York [2]. These events highlight the need for modeling approaches capable of capturing multi-sector interdependencies and supporting resilience-oriented decision-making.

Resilience – the ability to resist, absorb, adapt, and recover from disturbances – has become a cornerstone of modern CI protection [3]. Strengthening the resilience of essential services is a priority in international and European policy frameworks, including the Sendai Framework [4] and the Directive on the Resilience of Critical Entities (CER) [5]. The Horizon Europe project *MULTICLIMACT* contributes to these objectives by developing digital tools and standards to enhance preparedness and response across multiple hazard scenarios.

Within this context, the MARIS (Modeling infrAstructuRe dependencIes at urban Scale) methodology [6] provides an open-data-based approach for assessing the impact of natural and anthropogenic hazards on infrastructure systems. MARIS extends previous

* Corresponding author.
E-mail address: antonio.dipietro@enea.it (A. Di Pietro).

https://doi.org/10.1016/j.ijdrr.2025.105965
Received 29 August 2025; Received in revised form 11 December 2025; Accepted 13 December 2025
Available online 15 December 2025
2212-4209/© 2025 The Authors. Published by Elsevier Ltd. This is an open access article under the CC BY license (http://creativecommons.org/licenses/by/4.0/).

work [7] by explicitly incorporating failure propagation and short-term recovery controls into the risk assessment. Compared to its original formulation, the present version introduces a probabilistic and time-dependent representation of both disruption and recovery processes, enabling a quantitative evaluation of cascading effects across multiple CI sectors. The approach models how failures propagate through functional dependencies and how security controls – such as redundancy, protection devices, and automation – mitigate their effects and support rapid recovery. For example, during flood-induced disturbances in electric transmission systems, automated protection schemes and emergency interventions can significantly reduce outage durations and preserve service continuity. By integrating these mechanisms, MARIS evaluates both the spread of failures and the effectiveness of mitigation actions. Dependency Risk Graphs (DRGs) [8] provide the structural backbone of the methodology, encoding sectoral and POI-level dependencies through weighted links that represent propagation probabilities, impact magnitudes, and recovery activation. Open geospatial data (e.g., OSM Points of Interest) support the spatially explicit mapping of infrastructures and the identification of vulnerable subchains.

Early frameworks conceptualized CI interdependencies through static or deterministic representations [9–11], providing a foundation for later research. Despite substantial progress, existing approaches often fall short in their ability to quantify cascading effects dynamically and to integrate short-term recovery processes within probabilistic models. Most rely on fixed dependency structures, overlooking the uncertainty and temporal evolution of disruptions and recoveries. This limits the ability of decision-support systems to evaluate resilience in urban environments where heterogeneous infrastructures and open data must be combined. Recent studies have introduced temporal, stochastic, or multilayer network components to improve the realism of CI interdependency modeling [12–15]. However, these approaches often operate on abstract networks, treat disruption and recovery as decoupled processes, or rely on proprietary datasets, limiting their operational adoption by public authorities. Few existing frameworks jointly model the temporal evolution of disruptions, the mitigating influence of recovery actions, and the propagation of both processes along spatially explicit dependency chains. This motivates the need for an integrated, open-data-driven methodology for assessing dynamic resilience in real territorial contexts.

Accordingly, this work formulates three Research Problems (RPs), directly derived from the limitations identified above and aligned with current resilience policies:

RP1: How to model cascading failures across multiple CI sectors in a way that reflects both the structure and intensity of their functional interdependencies;

RP2: How to incorporate probabilistic recovery dynamics into dependency modeling, enabling a realistic representation of short-term resilience;

RP3: How to operationalize the methodology using primarily open data, ensuring transparency and reproducibility while acknowledging that some parameters rely on expert knowledge or literature-based assumptions.

Each Research Problem is addressed through a specific component of the extended MARIS framework. RP1 is addressed through a dependency-based representation of interdependent Critical Infrastructure sectors and assets, capturing both sectoral and asset-level interactions. RP2 focuses on the dynamic characterization of impact and recovery processes, enabling a probabilistic assessment of cascading effects and resilience over time. RP3 is addressed through an application to a real-world case study, demonstrating how the proposed methodology can be operationalized using predominantly open geospatial data complemented by expert-informed parameters.

To support operational deployment, the methodology has been integrated into the CIPCast Decision Support System [6], which enables continuous risk assessment for infrastructures exposed to natural and anthropogenic hazards. This integration allows public authorities and infrastructure operators to apply the MARIS framework for both ex-ante risk analysis and post-event decision-making, supporting the definition of measures aimed at enhancing systemic resilience. The methodology is applied to the municipality of Camerino–one of the MULTICLIMACT pilot sites and exposed to multiple natural hazards, including earthquakes–to demonstrate its operational applicability and provide actionable insights for resilience planning.

The remainder of this paper is structured as follows: Section 2 reviews related work; Section 3 presents the extended MARIS approach; Section 4 describes the Camerino case study; and Section 5 concludes the paper.

2. Related works

The MARIS methodology builds upon established research in *dependency network modeling*, *cascading failure analysis*, and *resilience assessment* of interdependent infrastructures. This review is organized thematically to identify the methodological gaps that motivate the extensions introduced in MARIS. Specifically, the literature is analyzed across four domains – dependency modeling, cascading failures, resilience assessment, and probabilistic/time-dependent approaches – highlighting for each domain the limitations that remain unresolved in current frameworks. This section highlights key methodological contributions and clarifies how MARIS extends current frameworks through dynamic failure-recovery modeling and POI-based spatial analysis.

In *dependency network modeling*, Yabe et al. [16] proposed a behavior-based dependency model for economic resilience, without explicitly representing infrastructure recovery. Wróbel [17] examined efficiency and susceptibility in networks, though without a quantitative propagation mechanism. Almoghathawi et al. [18] identified critical components but did not incorporate temporal cascading or recovery mitigation. Existing dependency-modeling approaches rarely integrate: (i) time-dependent propagation and recovery, (ii) probabilistic uncertainty, and (iii) spatially explicit POI-based modeling using open geospatial data. MARIS introduces all three components within a unified Dependency Risk Graph framework.

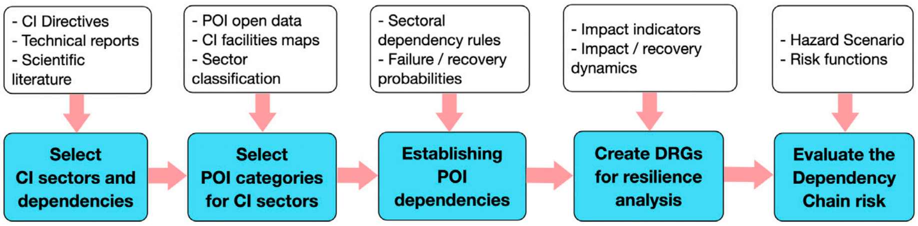

Fig. 1. Steps of the MARIS methodology.

Regarding *cascading failure analysis*, Theoharidou et al. [19] offered early conceptual models but limited to static topologies. Stergiopoulos et al. [20] included temporal dynamics, though without open-data spatial grounding. Shi et al. [21] proposed containment strategies for abstract networks, while Mbanaso et al. [22] used neural models whose interpretability limits operational applicability. Current cascading-failure models generally treat disruption as a dynamic process but not recovery; lack POI-level spatial grounding; and do not identify maximal dependency subchains in real territorial settings. MARIS explicitly models both disruption and recovery trajectories through directed acyclic paths and Monte Carlo simulations.

In *resilience modeling*, Akbarzadeh [23] addressed multi-order dependencies in cyber–physical systems, yet with limited physical-sector coupling. Zhang et al. [24] focused on diagnostics, detached from systemic propagation. Liu et al. [25] applied ML techniques without modeling cross-sector interactions or POI-level structures.

Fekete [26] introduced useful metrics such as critical proportion, time, and quality, which MARIS uses to enrich its impact-recovery modeling. These concepts help link service availability, disruption duration, and quality degradation, though they are not embedded within a cascading-propagation framework. Existing resilience frameworks do not provide a unified mechanism to quantify cross-sectoral cascading impacts, recovery dynamics, and POI-level spatial interactions. MARIS operationalises these elements by combining impact–recovery functions with open-data POI networks.

Finally, Tofani et al. [27] evaluated resilience in electrical distribution networks, with detailed sector-specific modeling but without inter-sector cascading dynamics, which MARIS explicitly incorporates. Across the three domains, the literature lacks a **probabilistic, time-dependent, and spatially explicit** model capable of representing both cascading failures and recovery processes at POI level. MARIS addresses this gap through: (1) open-data-based network construction, (2) weighted dependency modeling, and (3) Monte Carlo propagation of disruption and recovery along dependency chains.

Moreover, many existing frameworks depend on proprietary or non-reproducible datasets, limiting their operational use and transparent validation. This reinforces the need for an open-data-driven yet expert-informed approach such as MARIS, which balances reproducibility with realistic parameterization.

3. The MARIS methodology

This section extends the original MARIS framework [6] by integrating new methodological elements that were not present in the earlier version. Specifically, the revised formulation (i) introduces probabilistic parameters for both failure propagation and recovery activation, (ii) models their temporal evolution through impact and recovery functions, and (iii) embeds these within a multi-layer Dependency Risk Graph analyzed via Monte Carlo simulations.

The MARIS methodology provides a structured workflow for constructing and analyzing infrastructure dependency networks using open data. It is designed to identify the most critical interdependencies among infrastructures across sectors, assess their vulnerability to cascading failures, and quantify the evolving risk based on impact and recovery dynamics. By using POIs to localize these infrastructures, the methodology enables a more detailed representation of infrastructure dependencies, allowing for a precise mapping of how specific infrastructures rely on each other. This, in turn, enables decision-makers to prioritize mitigation strategies and enhance resilience during emergencies.

The approach proceeds by building a Dependency Relationship Graph (DRG) based on POI data. Initially, POIs are classified according to their associated critical infrastructure (CI) sectors. These classifications are then used to translate high-level sectoral dependencies into POI-level relationships. Finally, spatial and contextual criteria – such as geographic proximity – are applied to refine unknown or ambiguous links. The resulting DRG distinguishes between *consumer POIs*, which rely on external services, and *producer POIs*, which supply key resources or functionalities.

As illustrated in Fig. 1, the methodology is structured into a sequence of key steps, which are briefly summarized below and described in detail in the following subsections.

- **Step 1: Select CI Sectors and Dependencies**
  - Step 1a: Select CI sectors
  - Step 1b: Select CI dependencies
- **Step 2: Select POI categories for each CI sector**

Table 1
Step 1a: Critical infrastructure sectors under the CER directive [5].

CI sector	CI sector description
Energy	Electricity, oil, and gas sectors, focusing on production, distribution, and storage.
Transport	Road, rail, air, and water transport systems.
Banking	Essential services such as deposit taking and lending.
Financial Market Infrastructure	Services such as trading venues and clearing systems.
Health	Hospitals, medical facilities, and pharmaceutical supply chains.
Drinking Water	Supply and distribution of potable water.
Waste Water	Management and treatment of wastewater.
Digital Infrastructure	Telecommunications networks, data centers, and internet services.
Public Administration	Government services essential for public order and safety.
Space	Space-based services like satellite communication and navigation.
Food	Production, processing, and distribution of food products.

  - Step 2a: Select open data sources
  - Step 2b: Select POI categories
  - Step 2c: Extract POI intances

- **Step 3: Establish POI dependencies**
  - Step 3a: Define POI category dependencies
  - Step 3b: Define POI instance dependencies
  - Step 3c: Collect failure propagation and recovery action activation data
  - Step 3d: Adjust failure propagation and recovery action activation data with local modifiers

- **Step 4: Create Dependency Risk Graphs for resilience analysis**
  - Step 4a: Collect Impact and Recovery action metrics data
  - Step 4b: Adjust Impact and Recovery action metrics data with local modifiers
  - Step 4c: Create Dependency Risk Graphs

- **Step 5: Evaluate the Dependency Chain Risk**
  - Step 5a: Define the Dependency Chain Risk
  - Step 5b: Identify relevant subchains in the DRG
  - Step 5c: Evaluate the Dependency Chain Risk
  - Step 5d: Compare Dependency Risk across subchains in the DRG

In the following sections, each step of the MARIS methodology is examined in detail, providing a comprehensive explanation of its objectives, input data, and operational procedures involved in constructing the DRGs and assessing cascading risks.

3.1. Step 1 — select CI sectors and dependencies

Step 1 defines the system-level structure of the analysis by identifying the relevant Critical Infrastructure (CI) sectors and the functional dependencies linking them. This sectoral representation captures how disruptions may propagate across interconnected services, providing the conceptual basis for cascading impact analysis.

3.1.1. Step 1a — select CI sectors

Identifying the relevant Critical Infrastructure (CI) sectors is the first step in assessing interdependencies that may amplify the effects of disruptive events. We adopt the classification of the European Critical Entities Resilience (CER) Directive [5], which defines essential sectors such as energy, water, healthcare, transport, and digital infrastructure (Table 1). This ensures methodological consistency and policy relevance for resilience planning.

Alternative frameworks, such as the U.S. CISR Directive [28], may be used in other contexts, but this study follows the EU approach.

3.1.2. Step 1b — select CI dependencies

This step identifies the functional dependencies among the selected Critical Infrastructure (CI) sectors. A dependency is a relationship in which the operation of one sector relies on the availability or performance of another. These links may be physical (e.g., energy supply), informational (e.g., communication systems), or institutional (e.g., governance). Dependencies are not necessarily symmetric: a sector may rely on another without reciprocity. Mapping these interconnections is essential to assess potential cascading effects and system vulnerabilities.

Table 2 provides a representative set of inter-sector dependencies, adapted from ENISA's framework [29], and contextualized for our analysis.

3.2. Step 2: Select POI categories for each CI sector

Step 2 translates the sectoral dependency structure into a spatial representation by associating each CI sector with concrete Points of Interest (POIs). This step enables the transition from an abstract system model to a georeferenced asset-level representation suitable for impact assessment.

3.2.1. Step 2a: Select open data sources

To identify Points of Interest (POI) categories, it is essential to rely on a combination of open and restricted data sources. OpenStreetMap (OSM) is the primary open data source used in this study, offering a wide range of POI categories such as amenities, shops, transportation hubs, and infrastructure elements. These datasets are adaptable and allow for filtering by tags relevant to critical infrastructure sectors. However, open data may lack detail or completeness, especially for sensitive infrastructures. In such cases, supplementary data from CI operators or public authorities (e.g., municipal or national datasets) may be required to enhance coverage and accuracy.

3.2.2. Step 2b: Define POI categories

Based on the selected data sources – primarily OSM – POI categories are identified and linked to CI sectors (Table 3). This classification provides the basis for selecting the POI instances that populate the dependency network. Only categories consistent with the adopted CI-sector framework are retained, ensuring that the extracted data reflects the domains relevant for dependency modeling, such as energy, transport, health, and digital systems.

3.2.3. Step 2c: Extract POI instances

Once POI categories are defined, specific instances are extracted from the area of interest using geospatial tools such as the Overpass API. Each POI is then assigned to a CI sector based on its functional role; in some cases, facilities serving multiple functions (e.g., hospitals) require expert validation. The minimum information required includes the POI category, geographic location, functional dependencies, and – when relevant to the social dimension – the approximate number of users served.

3.3. Step 3: Establish POI dependencies

Once POI instances have been identified and associated with their corresponding CI sectors, the next step is to model the functional dependencies among them. This step builds upon the sector-level dependencies defined earlier and translates them into concrete relationships between individual infrastructure elements within the area of interest.

3.3.1. Step 3a: Define POI category dependencies

Sector-level CI dependencies must be translated into relationships between POI categories derived from OpenStreetMap. This mapping links high-level inter-sector dependencies to specific infrastructure types, enabling a granular representation of system interconnections.

For example, if the health sector depends on energy supply, hospitals are linked to power substations. Table 4 shows this correspondence and provides the basis for constructing the network of interdependent POIs.

3.3.2. Step 3b: Define POI instance dependencies

In this step, POI instances are connected according to the dependencies defined at the category level. Geographic proximity helps identify realistic links — for example, a hospital may depend on a nearby power substation for electricity. Mapping these dependencies at the POI level provides a detailed view of interconnections within the infrastructure network.

Table 2
Step 1b: Functional dependencies among CI sectors, reorganized according to the CER Directive [5] and adapted from ENISA [29].

CI sector	Depends on	Description of functional dependency
Energy	Transport	Fuel logistics and the transport of equipment depend on road, rail, or pipeline systems.
	Digital Infrastructure	Monitoring and control systems (e.g., SCADA) rely on ICT networks.
	Public Administration	Regulation, energy policy, and emergency management are state responsibilities.
Transport	Energy	Transportation networks depend on electricity and fuel for vehicles and operations.
	Digital Infrastructure	Traffic management, navigation, and logistics systems require ICT.
	Public Administration	Infrastructure planning, safety regulations, and public coordination are governed by authorities.
Banking	Digital Infrastructure	Electronic transactions and banking platforms require reliable ICT services.
	Energy	Banks and ATMs need continuous power to operate securely.
	Public Administration	Supervision, compliance, and monetary policy are handled by state institutions.
Financial Market Infrastructure	Digital Infrastructure	Trading systems and clearing platforms depend on stable, secure ICT networks.
	Energy	Data centers and trading floors rely on uninterrupted energy supply.
	Public Administration	Regulatory frameworks and risk oversight are managed by public authorities.
Health	Energy	Medical facilities require constant energy for equipment and emergency services.
	Digital Infrastructure	Health IT systems, diagnostics, and telemedicine depend on ICT.
	Drinking Water	Clean water is essential for hygiene, treatment, and patient care.
	Transport	Ambulance services and medical logistics depend on functional transport infrastructure.
	Public Administration	Governance, funding, and health policies are under public jurisdiction.
Drinking Water	Energy	Pumping, purification, and distribution systems are electrically powered.
	Digital Infrastructure	Remote monitoring and quality control use digital systems.
	Public Administration	Water safety regulations and contingency planning are state-managed.
Waste Water	Energy	Treatment plants and sewage systems depend on continuous electricity.
	Digital Infrastructure	Supervisory and automation systems operate through ICT infrastructure.
	Public Administration	Wastewater standards and environmental controls are established by public authorities.
Digital Infrastructure	Energy	Data centers, servers, and network infrastructure require continuous power.
	Transport	Deployment and maintenance of hardware require transport logistics.
	Public Administration	Regulation, licensing, and cybersecurity oversight fall under government authority.
Public Administration	Digital Infrastructure	E-government services and digital records require ICT.
	Energy	Administrative buildings and services rely on stable energy.
Space	Energy	Satellite systems and ground control centers require reliable energy supply.
	Digital Infrastructure	Space operations depend on telecommunication and data transmission networks.
	Public Administration	Space activities are regulated, funded, and coordinated by public institutions.
Food	Transport	Food distribution chains rely on functional transport networks.
	Energy	Food processing, storage, and retail facilities depend on electrical energy.
	Digital Infrastructure	Supply-chain management, traceability, and digital payment systems depend on ICT.
	Public Administration	Food safety, inspection systems, and emergency logistics are under public governance.

Table 3
Step 2b: A possibile association between Critical Infrastructure (CI) sectors and OpenStreetMap (OSM) categories. Each category is represented as a key–value pair (`key=value`), where the equals sign denotes the attribute-value relationship used in OSM to tag features (e.g., `amenity=hospital`).

CI sector	OSM categories	Explanation
Energy	power=substation, power=generator, power=plant, power=line	Facilities and infrastructure related to electricity generation, transmission, and distribution.
Transport	highway=bus_stop, railway=station, aeroway=aerodrome, amenity=ferry_terminal	Transportation hubs and infrastructure for various modes of transport such as road, rail, air, and water.
Banking and Financial Market	amenity=bank, amenity=atm, office=financial	Locations of banks, ATMs, and financial offices.
Health	amenity=hospital, amenity=clinic, amenity=pharmacy	Health facilities providing medical services and pharmaceuticals.
Drinking water	man_made=water_tower, amenity=drinking_water, natural=spring	Infrastructure and natural sources providing drinking water.
Waste water	man_made=wastewater_plant, water=reservoir	Facilities involved in wastewater treatment and management.
Digital Infrastructure	man_made=communication_tower, office=telecommunication	Communication infrastructure like towers and telecommunication offices.
Public Administration	amenity=townhall, office=government	Government offices and administrative buildings.
Space	man_made=launchpad, spaceport	Space-related infrastructure such as launchpads and spaceports.
Food	shop=supermarket, amenity=restaurant, amenity=fast_food	Places where food is sold or served, including supermarkets and eateries.

3.3.3. Step 3c: Collect failure propagation and recovery action activation data

This step quantifies the probability that a failure in a provider infrastructure (v_j) causes a disruption in a dependent consumer infrastructure (v_k). Following classical reliability frameworks [30,31], the failure propagation probability $L_{j,k}$ is defined as the conditional probability that the failure of v_j triggers a functional loss in v_k:

$$L_{j,k} = P(F_k, |, F_j) \tag{1}$$

where F_j and F_k denote the failure states of the provider and consumer infrastructures. It may be estimated through FTA/ETA or, when data exist, from observed joint failures:

$$L_{j,k} = \frac{N(F_j \cap F_k)}{N(F_j)} \tag{2}$$

The recovery activation probability $\bar{L}j,k$ expresses the likelihood that a recovery measure (e.g., backup power) is activated following a failure:

$$\bar{L}j,k = P(R_k, |, F_j) \tag{3}$$

Both $L_{j,k}$ and $\bar{L}_{j,k}$ range in $[0,1]$ and provide the probabilistic inputs for the risk propagation model, enabling a combined representation of failure spread and recovery effectiveness.

3.3.4. Step 3d: Adjust failure propagation and recovery action activation data with local modifiers

This step refines failure propagation and recovery activation probabilities by incorporating local modifiers that account for context-specific conditions. These factors include:

- **Geographical proximity**: distance between infrastructures, affecting propagation likelihood and recovery times.
- **Redundancy and backup systems**: alternative supply or protection measures that reduce vulnerability.
- **Environmental conditions**: local hazards or terrain influencing disruption and recovery.
- **Infrastructure quality**: condition and maintenance level affecting susceptibility and response efficiency.
- **Regulatory and safety measures**: local rules and practices that enhance resilience.
- **Other locally relevant infrastructures**: assets not listed as CI in ENISA or CER (e.g., municipal utilities, schools used as shelters, civil protection depots) that shape cascading effects and coordinated recovery.

These modifiers enable a more context-sensitive estimation of failure and recovery probabilities.

Table 4
Step 3a: Revised POI category dependencies including multiple linkages with `amenity=townhall`, reflecting the coordination and regulatory role of Public Administration across sectors.

CI sector	POI consumer	POI provider	POI provider motivation
Energy	power=substation	highway=bus_stop power=line	For maintenance and operational staff Connectivity to the power grid
Transport	railway=station	power=plant shop=supermarket	Power for station operations Access to food and supplies for travelers
Banking and Financial Market	amenity=bank	power=plant man_made=communication_tower amenity=townhall	Power supply for secure operations Digital connectivity for transactions Regulatory and oversight functions
Health	amenity=hospital	power=generator amenity=drinking_water amenity=townhall	Backup power supply Clean water supply Administrative coordination for emergency response
Drinking water	man_made=water_tower	power=plant amenity=townhall	Electricity for pumping and distribution Regulation, planning, and management
Waste water	water=reservoir	power=substation man_made=wastewater_plant amenity=townhall	Electricity for pumping and maintenance Inflow of treated water Environmental regulation and monitoring
Digital Infrastructure	man_made= communication._tower	power=generator office=government	Backup power supply Regulation and oversight
Public Administration	amenity=townhall	power=substation highway=bus_stop	Electricity for operations Accessibility for citizens and staff
Space	man_made=launchpad	power=substation aeroway=aerodrome	Electricity for launch operations Transportation of personnel and equipment
Food	shop=supermarket	power=substation amenity=restaurant amenity=townhall	Electricity for refrigeration and operations Supply chain for food items Food safety and inspection authority

3.4. Step 4: Create dependency risk graphs for resilience analysis

Building on the sector-level dependency framework discussed in the previous section, the following subsections illustrate how these relationships are translated at the POI level and parameterized in order to construct the Dependency Risk Graph (DRG) used in the MARIS workflow.

3.4.1. Step 4a: Collect impact and recovery action metrics data

In this phase, the focus is on modeling the metrics for both impact and recovery actions for each dependency between Points of Interest (POIs). The goal is to quantify the intensity, maximum value, time to reach the maximum value, and growth rates for both impact and recovery, evaluated across societal, economic, and operational dimensions, within the context of natural and anthropogenic threats.

Building on Fekete's framework [26], which accounts for time-dependent aspects of disruptions, impact is defined as the disruption caused to services or infrastructure, including severity and duration. Recovery, conversely, represents the reduction in impact over time, reflecting the system's ability to mitigate and reverse the effects through recovery actions.

For both impact and recovery, three key indicators are used for each POI category: societal impact (the number of people affected by POI unavailability), economic impact (GDP loss), and operational impact (reduction in capacity). Recovery is modeled using the same parameters as impact: the maximum recovery value, the time to reach that maximum, and the growth rate, describing how effectively and quickly the system mitigates the disruption.

Thus, while impact quantifies the severity of the disruption, recovery represents the system's capacity to restore functionality, progressively reducing the impact over time.

To model the time-dependent dynamics of impact and recovery for two generic POI instances, j and k, and to evaluate the impact on k due to the unavailability of j, we define the *generic impact function* $I_{j,k}(t)$ as follows:

$$I_{j,k}(t) = \begin{cases} M_{j,k} \cdot \left(\frac{t}{T_{j,k}} \right)^2 & \text{if } U_{j,k} = 1 \text{ (slow)} \\ M_{j,k} \cdot \left(\frac{t}{T_{j,k}} \right) & \text{if } U_{j,k} = 2 \text{ (linear)} \\ M_{j,k} \cdot \frac{\log(t+1)}{\log(T_{j,k}+1)} & \text{if } U_{j,k} = 3 \text{ (fast)} \end{cases} \tag{4}$$

In this formulation, the parameters $M_{j,k}$, $T_{j,k}$, and $U_{j,k}$ represent the maximum impact of the failure of infrastructure j on k, the time required to reach this maximum, and the type of temporal growth (slow, linear, or fast), respectively. The three alternative functions in Eq. (4) allow the model to capture different propagation dynamics: slow quadratic growth for gradual degradations, linear for steady deterioration, and logarithmic for fast-onset cascading effects such as communication or power outages. Compared with the exponential-type formulations proposed in [7], these polynomial and logarithmic trends ensure bounded behavior and numerical stability when simulating multiple interdependent chains. The parameter $T_{j,k}$ is capped at four weeks, consistent with the temporal resolution adopted in the MARIS analyses.

The recovery function, analogous to the impact function, describes the recovery process over time. Recovery follows the same growth patterns (slow, linear, fast) but focuses on how quickly and effectively the system mitigates the effects of disruption.

The time-dependent functions of impact and recovery between two POI instances j and k are given by suitable functions of t, $M_{j,k}$, $U_{j,k}$, $T_{j,k}$ and t, $\bar{M}_{j,k}$, $\bar{U}_{j,k}$, $\bar{T}_{j,k}$, respectively:

$$I_{j,k}(t) = I_{j,k}(t, M_{j,k}, U_{j,k}, T_{j,k})$$
$$\bar{I}_{j,k}(t) = \bar{I}_{j,k}(t, \bar{M}_{j,k}, \bar{U}_{j,k}, \bar{T}_{j,k}).$$

The variables above are assigned from the following Likert scales:

- $M_{j,k}, \bar{M}_{j,k} \in [1..8]$: impact and recovery scale, from minimal (1) to maximal (8) severity.
- $T_{j,k}$, $\bar{T}_{j,k}$, $t \in \mathcal{T}$, with $\mathcal{T} = \{t_1, \ldots, t_9\}$, $t_1 = 15$ min, $t_2 = 1$ h, $t_3 = 3$ h, $t_4 = 12$ h, $t_5 = 24$ h, $t_6 = 48$ h, $t_7 = 1$ w, $t_8 = 2$ w, $t_9 = 4$ w: discrete time scale representing the duration of unavailability or recovery.
- $U_{j,k}, \bar{U}_{j,k} \in \{1, 2, 3\}$: growth patterns: 1 (slow), 2 (linear), 3 (fast).

Here, $M_{j,k}$ and $\bar{M}_{j,k}$ represent the maximum intensity of impact and recovery, respectively; $T_{j,k}$ and $\bar{T}_{j,k}$ denote the time required for impact or recovery to reach its maximum level; and $U_{j,k}$ and $\bar{U}_{j,k}$ specify the growth pattern of the corresponding function.

By assigning these three characteristic parameters to each dependency between POI instances, it is possible to model both the escalation of impact and the effectiveness of recovery over time, enabling a dynamic and granular assessment of infrastructure resilience.

3.4.2. Step 4b: Adjust impact and recovery metrics with local modifiers

At this stage, the previously derived impact and recovery metrics are refined by incorporating local modifiers that capture the geographical, environmental, and infrastructural context. These factors may influence the key properties of impact and recovery – *impact value*, *time to maximum impact*, and *growth rate* – depending on the specific characteristics of the area under analysis. The main modifiers include the *geographical context* (spatial distribution, accessibility, and population density), *demographic variations* (presence of vulnerable groups and socio-economic conditions that can amplify disruption severity, as socially fragile communities often experience higher *impact values* due to unequal access to services and resources; see [32]), and *environmental conditions* (climate, exposure to natural hazards, and terrain morphology). Additional factors such as *redundancy and backup systems*, *infrastructure quality and maintenance*, and *regulatory and safety measures* can also modify the intensity or duration of disruption. In practice, these modifiers are applied through simple multiplicative or additive correction factors to the baseline parameters $M_{j,k}$, $T_{j,k}$ and $U_{j,k}$, ensuring that the adjusted values remain within the same ordinal Likert scale while reflecting case-specific attributes (e.g., mountain terrain may increase $T_{j,k}$, whereas high redundancy in utility networks may reduce $M_{j,k}$).

3.4.3. Step 4c: Create dependency risk graphs

The *Dependency Risk Graph* (DRG) represents the structural and functional interconnections among Points of Interest (POI) instances within a given area. Based on the outcomes of the previous methodological steps, this graph is instantiated using the identified POI instances as nodes and their functional dependencies as directed edges. To capture the propagation of disruptions across the three considered dimensions – *social*, *economic*, and *operational* – the DRG is defined in three distinct variants, each weighted to reflect the specific characteristics and severity of the corresponding impact type.

Accordingly, we define three Dependency Risk Graphs: $G^s = (V, E, W^s)$, $G^e = (V, E, W^e)$, and $G^o = (V, E, W^o)$, representing the social, economic, and operational perspectives, respectively. While the node set V and edge set E remain consistent across all graphs – capturing the common structural layout – the associated weight sets W^s, W^e, and W^o differ, as they encode dimension-specific impact and recovery parameters. For example, social impact may emphasize emergency response and population protection, whereas operational impact is more concerned with infrastructure continuity and system functionality.

In the remainder of this section, the structure of the generic weighted Dependency Risk Graph $\hat{G}$ is described, as defined in Eq. (5), which represents any of the three graphs introduced below.

$$\hat{G} = (V, E, W) \tag{5}$$

- $V = \{v_k\}$ is the set of POI instances specific to the area of interest (**Step 2b**);
- $E = \{e_{jk}\}$ is the set of directed edges representing dependencies between POI instances (**Step 2c**);
- $W = \{\mathbb{L}, \bar{\mathbb{L}}, \mathbb{I}, \bar{\mathbb{I}}, \mathbb{T}, \bar{\mathbb{T}}, \mathbb{U}, \bar{\mathbb{U}}\}$ is the set of weight parameters associated with each edge $e_{jk} \in E$.

Each component of W is defined as follows:

- $\mathbb{L} = \{L_{j,k}\}$: likelihood that a disruption at node v_j propagates to node v_k (**Steps 3c, 3d**);
- $\bar{\mathbb{L}} = \{\bar{L}_{j,k}\}$: effectiveness of recovery actions at node v_k in mitigating the impact propagated from node v_j (**Steps 3c, 3d**);
- $\mathbb{I} = \{M_{j,k}\}$: maximum potential impact on node v_k due to the failure of node v_j (**Steps 4a, 4b**);
- $\bar{\mathbb{I}} = \{\bar{M}_{j,k}\}$: maximum potential recovery effect on node v_k resulting from actions taken on v_j (**Steps 4a, 4b**);
- $\mathbb{T} = \{T_{j,k}\}$: time required for the impact from v_j to reach its peak on v_k (**Steps 4a, 4b**);
- $\bar{\mathbb{T}} = \{\bar{T}_{j,k}\}$: time required for recovery effects initiated at v_j to become fully effective on v_k (**Steps 4a, 4b**);
- $\mathbb{U} = \{U_{j,k}\}$: impact growth pattern (1 = slow, 2 = linear, 3 = fast) (**Steps 4a, 4b**);
- $\bar{\mathbb{U}} = \{\bar{U}_{j,k}\}$: recovery growth pattern (same scale as U) (**Steps 4a, 4b**).

This representation enables a unified modeling framework for evaluating risk propagation and recovery dynamics across different impact types, supporting indicator-specific resilience analysis.

3.5. Step 5: Evaluate the dependency chain risk

Step 5 evaluates cascading risk propagation along dependency chains in the Dependency Risk Graph by integrating failure likelihoods, impact functions, and recovery dynamics, enabling the assessment and comparison of critical paths in terms of risk and resilience.

3.5.1. Step 5a: Define the dependency chain risk

To assess the risk of cascading failures, consider a generic Dependency Risk Graph $\hat{G}$ as defined in Eq. (5), and a dependency chain represented as a sequence of nodes within the graph. Let C^{ℓ} denote a dependency chain composed of $\ell + 1$ nodes and ℓ directed edges, formally defined as:

$$C^{\ell} = (v_0, v_1, \dots, v_{\ell}), \quad (v_{i-1}, v_i) \in E \;\; \forall i = 1, \dots, \ell. \tag{6}$$

The formulation assumes that C^{ℓ} is a *directed acyclic path (DAP)*, a linear non-branching sequence of nodes connected by directed edges [33]. This assumption excludes cycles or branching dependencies and allows the model to compute propagation effects along tractable acyclic paths.

The *cumulative dependency risk* function, which incorporates the effects of recovery actions, is defined as follows:

$$\widetilde{D}_{C^{\ell}}(t) = \sum_{j=1}^{\ell+1} \left[\left(\prod_{k=1}^{j} L_{k-1,k} \right) \cdot I_{j-1,j}(t) - \left(\prod_{k=1}^{j} \bar{L}_{k-1,k} \right) \cdot \bar{I}_{j-1,j}(t) \right] \tag{7}$$

Eq. (7) quantifies the time-dependent difference between unmitigated and mitigated risks, accounting for failure propagation and recovery effects along dependency chains. The total risk is computed as the sum of contributions over all acyclic paths. This linear approximation allows for scalable representation of systemic risk, while acknowledging that real-world cascading effects may involve nonlinear dynamics that are abstracted in this formulation.

To ensure consistent representation of cascading dynamics, non–negativity is imposed after aggregating the cumulative risk along a complete dependency chain. This constraint allows recovery effects at upstream nodes to mitigate downstream impacts, ensuring the final risk is bounded from below:

$$D_{C^{\ell}}(t) = \max\left(0, \widetilde{D}_{C^{\ell}}(t)\right) \tag{8}$$

3.5.2. Step 5b: Identify relevant subchains in the DRG

In this step, we identify the set of Points of Interest (POIs) directly affected by an external disruption, either natural or anthropogenic. These POIs are assumed to be in a failed state, forming the **Scenario Failure Set**:

$$V_F = \{v_f \in V \mid v_f \text{ is in a failed state at time } t_0\}.$$

The objective is to extract from the Dependency Risk Graph (DRG) all directed paths that may propagate the disruption. Each path is a simple (acyclic) sequence of nodes with length strictly smaller than the **Maximum Path Length** ℓ, which defines the structural depth of the analysis. In this context, the terms *subchain* and *path* are used interchangeably.

Based on Eq. (6), the set of relevant subchains, denoted as the **Critical Path Set**, is defined as

$$\mathcal{S}_{\ell,V_F} = \left\{ C^n \;\middle|\; C^n \subseteq C^\ell,\ C^n \text{ acyclic},\ n < \ell,\ \exists v_i \in C^n \cap V_F \right\}. \tag{9}$$

Thus, $\mathcal{S}_{\ell,V_F}$ contains all acyclic subchains of length smaller than ℓ that include at least one failed POI from V_F. To avoid redundancy, only maximal subchains are retained, i.e., those not strictly contained in any longer subchain of the same set. Formally, for each $C^n \in S(\ell, V_F)$:

$$\forall C^m \in \mathcal{S}_{\ell,V_F},\ \left(m > n \;\Rightarrow\; C^n \nsubseteq C^m\right).$$

This ensures that $\mathcal{S}_{\ell,V_F}$ contains only structurally independent paths, focusing the analysis on those most relevant for cascading propagation.

As noted by König (2020), failures tend to lose influence along long dependency paths. For analytical and computational efficiency, subchains are therefore limited to a maximum length ℓ. Restricting the analysis to these bounded acyclic paths enables an interpretable and precise assessment of disruption propagation, helping to identify critical paths and guide resilience strategies.

3.5.3. Step 5c: Evaluate the dependency chain risk

In this step, the *Cumulative Dependency Risk* functions are evaluated for each subchain in the Critical Path Set $\mathcal{S}_{\ell,V_F}$. The assessment is performed independently for the economic, social, and operational DRGs. For clarity, the formal definition is presented for a single impact dimension, with the same procedure applying to the others. The cumulative risk of a subchain is obtained by aggregating failure propagation and recovery effects along its edges, based on the corresponding *weight set* W.

To account for uncertainty, a Monte Carlo framework is used. For each subchain $C_i^\ell \in \mathcal{S}_{\ell,V_F}$, where $i = 1, \dots, B$ and $B = |\mathcal{S}_{\ell,V_F}|$, the cumulative risk is evaluated over Q simulation runs. At each iteration $r = 1, \dots, Q$, input parameters – impact and recovery distributions – are independently sampled from their probability laws.

The risk function[1] for a single realization, originally defined in Eqs. (7) and (8), can be reformulated for a generic subchain C_i^ℓ as follows:

$$\widetilde{D}_{C_i^\ell}(t) = \sum_{j=1}^{\ell} \left[\left(\prod_{k=1}^{j} L_{k-1,k} \right) \cdot I_{j-1,j}(t) - \left(\prod_{k=1}^{j} \bar{L}_{k-1,k} \right) \cdot \bar{I}_{j-1,j}(t) \right] \tag{10}$$

$$\mathbb{D}_{C_i^\ell}(t) = \max\left(0, \widetilde{D}_{C_i^\ell}(t)\right). \tag{11}$$

As previously defined, let $\mathcal{T}$ be the discrete time scale (with $|\mathcal{T}| = 9$). For each subchain $C_i^\ell \in \mathcal{S}_{\ell,V_F}$, the Monte Carlo simulation provides Q independent realizations of the normalized cumulative risk $\mathbb{D}^{(r)}_{C_i^\ell}(t)$, with $t \in \mathcal{T}$ and $r = 1, \dots, Q$. The expected value at time t is

$$\overline{\mathbb{D}}_{C_i^\ell}(t) = \frac{1}{Q} \sum_{r=1}^{Q} \mathbb{D}^{(r)}_{C_i^\ell}(t), \quad t \in \mathcal{T}. \tag{12}$$

By aggregating the expected values across all subchains in $\mathcal{S}_{\ell,V_F}$, we obtain:

$$\overline{\mathbb{D}}_{\mathcal{S}_{\ell,V_F}}(t) = \left\{ \overline{\mathbb{D}}_{C_1^\ell}(t), \overline{\mathbb{D}}_{C_2^\ell}(t), \dots, \overline{\mathbb{D}}_{C_B^\ell}(t) \right\}, \quad t \in \mathcal{T}. \tag{13}$$

This formulation clarifies that the set of mean cumulative risks $\overline{\mathbb{D}}_{\mathcal{S}_{\ell,V_F}}(t)$ is associated with the specific Critical Path Set generated by the chosen Scenario Failure Set V_F.

3.5.4. Step 5d: Compare dependency risk across subchains in the DRG

In the previous step, for each subchain C_i^ℓ in the *Critical Path Set*, the mean cumulative dependency risk $\overline{\mathbb{D}}_{C_i^\ell}(t)$ was obtained to describe the time-dependent effects of failure propagation and recovery. Since these temporal functions are not directly comparable across subchains, a scalar resilience metric is introduced.

This metric captures the severity and duration of disruptions together with the system's recovery capability. The *resilience* of a subchain C_i^ℓ, expressed as a percentage, is defined as:

$$\mathbb{R}_{C_i^\ell} = \left(1 - \frac{1}{K_\ell} \int_{\mathcal{T}} \overline{\mathbb{D}}_{C_i^\ell}(t)\, dt\right) \cdot 100, \tag{14}$$

where:

- $\overline{\mathbb{D}}_{C_i^\ell}(t)$ is the mean cumulative dependency risk at time t;
- $K_\ell = I_{\max} \cdot \ell \cdot |\mathcal{T}|$ is the worst-case cumulative disruption (with $I_{\max} = 8$, see Section 3.4.1);
- $\mathcal{T}$ is the discrete time horizon of disruption and recovery.

[1] Risk is treated as dimensionless to allow comparison across sectors.

This normalization bounds resilience within $[0, 100]$: lower values indicate more intense or prolonged disruption, while higher values reflect faster or more effective recovery influenced by redundancy, absorption capacity, or weaker interdependencies.

Applying Eq. (14) to each subchain in S_{ℓ,V_F} yields the *Resilience Values Set*:

$$\mathbb{R}_{S_{\ell,V_F}} = \left\{ \mathbb{R}_{C_1^\ell}, \mathbb{R}_{C_2^\ell}, \dots, \mathbb{R}_{C_B^\ell} \right\}. \tag{15}$$

This set enables comparison across subchains: lower values identify less resilient (more vulnerable) paths, whereas higher values denote subchains where disruptions are less likely to propagate or are mitigated more effectively. The distribution of $\mathbb{R}_{S_{\ell,V_F}}$ supports the ranking of critical paths and informs mitigation and protection strategies across interdependent CI systems.

4. Case study: The city of Camerino

This section applies the MARIS methodology to a real territorial context, focusing on the scenario-specific elements of each step.

The case study concerns the city of Camerino, a historical town in the Marche region severely affected by the 2016 Central Italy earthquake. The presence of the University of Camerino (UNICAM), together with the city's dense historical fabric and essential urban services, makes it an appropriate context for analyzing cascading risk propagation and the resilience of interdependent infrastructures.

4.1. Step 1: Select CI sectors and dependencies

Following the general procedure defined in Section 3, the analysis for Camerino focused on the CI sectors most relevant to a seismically exposed mid-sized town.

4.1.1. Step 1a: Select CI sectors

Considering the city of Camerino, the most relevant infrastructure subsets include public administration – responsible for territorial management and emergency coordination – and the health sector, supported by local healthcare facilities that proved crucial after the 2016 earthquake. Digital infrastructure also plays a key role due to the presence of the University of Camerino (UNICAM), which depends on reliable telecommunications for research and education. Water supply and management are equally important, especially given the area's seismic vulnerability, while the local road network, though limited, is essential for access to services and emergency response.

Other sectors such as energy and food remain part of the analysis but are not uniquely distinctive in Camerino. The selected sectors and their interdependencies (Step 1b) are summarized in Table 5, ensuring consistency between sector selection and dependency modeling.

While the classification follows the EU CER Directive, contextual adjustments were made. Drinking and waste water were merged due to shared management practices; Emergency Services and Commercial Facilities were included for local relevance; and sectors such as Space and Financial Markets were excluded because they play no significant operational role in Camerino.

4.1.2. Step 1b: Select CI dependencies

For the city of Camerino, the most relevant Critical Infrastructure (CI) sectors and their interdependencies are summarized in Table 5, complementing the sector selection introduced in Step 1a. The table outlines the key dependency relationships among sectors, with particular emphasis on energy, digital services, water systems, and public administration — core components for ensuring functionality and emergency coordination in a seismically active and structurally complex urban context such as Camerino.

4.2. Step 2: Select POI categories for each CI sector

In this section, we apply the MARIS POI-based workflow to the Camerino context, detailing the extraction and classification of locally relevant infrastructure elements from open geospatial data.

4.2.1. Step 2a: Select open data sources

For the identification of Points of Interest (POIs) in the Camerino area, OpenStreetMap (OSM) was adopted as the primary open data source, owing to its detailed representation of key urban and infrastructural elements such as public buildings, health and emergency services, and mobility nodes. In Camerino, OSM provides a solid baseline for mapping most essential facilities — including the University of Camerino, the municipal hospital, police stations, and water supply structures.

However, data completeness is not uniform across all categories: some infrastructures, particularly utility-related or civil protection assets, are underrepresented. To address these gaps, OSM data was complemented with municipal records and targeted field verification, ensuring adequate coverage and accuracy for the purposes of dependency modeling.

4.2.2. Step 2b: Define POI categories

The POI categories were primarily derived OSM tag taxonomies and selected according to their coherence with the CI sectors considered in this study, as well as their expected presence in the urban context of Camerino (Table 6).

These categories were selected to ensure compatibility with the CI sector classification used in our model and to reflect the specific infrastructural and functional characteristics of the Camerino urban area.

Table 5
Steps 1a and 1b: Relevant CI Sectors and Dependencies for Camerino. X indicates sectors under the EU CER Directive.

CI Sector	CER	Depends On	Dependency Description
Energy	X	Public Administration Digital Infrastructure	Regulatory frameworks and emergency protocols. Smart grids and energy management systems.
Transport	X	Energy Digital Infrastructure Public Administration	Fuel and power for vehicles and roads. Traffic and logistics optimization. Policy and maintenance coordination.
Banking	X	Energy Digital Infrastructure	Power for branches and ATMs. Core and online banking operations.
Health	X	Energy Drinking & Wastewater	Power for hospitals and equipment. Water for hygiene and medical procedures.
Drinking & Wastewater	X	Energy Public Administration	Treatment and distribution operations. Oversight and emergency provision.
Digital Infrastructure	X	Energy Public Administration	Networks and ICT systems. E-government and digital services.
Public Administration	X	All Sectors	Regulation, policy, emergency coordination.
Food	X	Energy Public Administration	Refrigeration, storage, and transport. Safety and crisis regulations.
Commercial Facilities		Energy Public Administration	Operations and utilities. Safety and regulatory enforcement.
Emergency Services		Energy Drinking & Wastewater Digital Infrastructure	Communications and life-support. Sanitation and firefighting. Coordination and dispatch systems.

Table 6
Mapping between CI sectors and OSM POI categories relevant to the Camerino case study.

CI sector	Subsector tags	Relevant OSM categories
Public Administration	Townhall, University, Government Office	`amenity=townhall`, `amenity=university`, `office=government`
Emergency Services	Police Station, Fire Station, Ambulance Station	`amenity=police`, `amenity=fire station`, `amenity=ambulance station`
Health	Hospital, Clinic, Doctor, Pharmacy	`amenity=hospital`, `amenity=clinic`, `amenity=doctors`, `amenity=pharmacy`
Banking Services	Bank, ATM, Financial Office	`amenity=bank`, `amenity=atm`, `office=financial`
Drinking Water and Wastewater	Water Tower, Spring, Drinking Water Tap	`man made=water tower`, `natural=spring`, `amenity=drinking water`
Digital Infrastructure	Communication Tower, Telecom Office	`man made=communications tower`, `office=telecommunication`
Food Supply and Commercial Services	Supermarket, Restaurant, Fast Food	`shop=supermarket`, `amenity=restaurant`, `amenity=fast food`
Transport Infrastructure	Bus Stop, Train Station	`highway=bus stop`, `railway=station`
Energy Infrastructure	Substation, Power Plant, Power Line	`power=substation`, `power=plant`, `power=line`

4.2.3. Step 2c: Extract POI instances

The selected area corresponds to a circular zone with a 1 km radius (approximately 3.14 km^2), encompassing the core of the city's urban and institutional fabric. The extraction was performed using the Overpass API and filtered according to the OSM tags identified in the previous step. Additional POIs were integrated from datasets provided by the Municipality of Camerino, ensuring consistency with local infrastructure records and institutional priorities.

Each POI instance was then assigned to the corresponding CI sector based on its functional role. For instance:

- **Public Administration**: *Palazzo Ducale*, *University of Camerino*, *Nuovo Studentato Montagnano*.
- **Emergency Services**: *Polizia Municipale*, *Carabinieri*, *Croce Rossa Italiana*.
- **Healthcare**: *Santa Maria della Pietà Hospital*, *Centro di Salute Mentale*.
- **Banking Services**: *Bank*, *ATM Intesa Sanpaolo*.
- **Water & Wastewater**: *Serbatoio Sellano*, *Serbatoio Servola*, *Serbatoio Torrone-San Gregorio*, *Fountains*.

Table 7
Step 2c: Assignment of POI instances to critical infrastructure sectors in Camerino, aligned with the sector order of Table 5.

Assigned CI sector	Relevant POI	Total POIs
Energy	Power Supply Systems, Energy Distribution Points	3
Transport	Main Roads, Local Transport Infrastructure	8
Banking	Bank, ATM Intesa Sanpaolo	13
Health	Local Hospital (e.g., Santa Maria della Pietà, Area Vasta 3 Pronto Soccorso)	31
Drinking & Waste water	Serbatoio Sellano, Serbatoio Servola, Serbatoio Torrone-San Gregorio	28
Digital Infrastructure	Internet Connection Point	4
Public Administration	Palazzo Ducale, University of Camerino, Nuovo Studentato Montagnano, Centro Universitario Sportivo	66
Food	Local markets, grocery stores, agricultural businesses, and restaurants (e.g., Supermercato Maxi Coal Maddalena)	114
Commercial Facilities	Chiesa di San Severo, Centro Universitario Sportivo	336
Emergency Services	Polizia Municipale, Carabinieri, Croce Rossa Italiana	11
Total		**614**

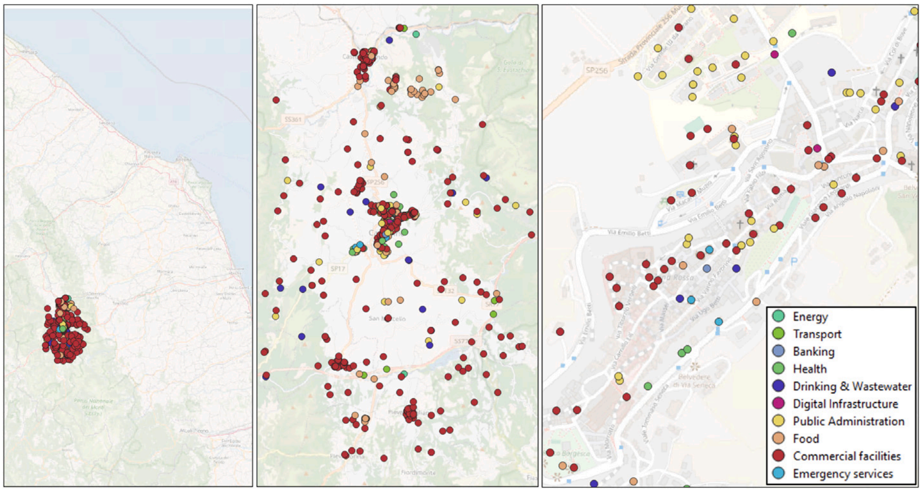

Fig. 2. Step 2c: Multi-scale visualization of POIs in Camerino across critical infrastructure sectors, from left to right: regional context, municipal area, and historical center.

- **Digital Infrastructure**: *Internet Connection Point*.
- **Commercial Facilities and Food**: *Supermercato Maxi Coal Maddalena*, *Local restaurants*, *Chiesa di San Severo*, *Centro Universitario Sportivo*.
- **Transport**: *Main roads*, *Bus stops*.
- **Energy**: *Power Supply Systems*, *Energy Distribution Points*.

In total, 614 POI instances were identified and classified, forming the basis for the construction of the dependency graph across CI sectors in Camerino. A detailed summary of the distribution is reported in Table 7 and a map of POI instances is shown in Fig. 2.

4.3. Step 3: Establish POI dependencies

Building on the POI classification, this section defines functional dependencies between instances. Dependencies are derived from sector-level relationships and spatial proximity, and are quantified through probabilistic parameters of failure propagation and recovery, refined by local modifiers.

Table 8
Step 3a: POI category dependencies by sector, consistent with Table 5.

Sector	Subsector dependent	Subsector providers	Dependencies
Energy	Substation	Connection Point, Communication Tower	2
Transportation	Motorway Junction, Aerodrome	Substation, Water Tower, Wastewater Plant, Police, Hospital, Communication Points	11
Banking	Bank, ATM, Payment Terminal	Substation, Water Tower, Wastewater Plant, Communication Towers	18
Health	Hospital, Clinic, Pharmacy	Substation, Water Tower, Wastewater Plant, Ambulance Station, Communication Towers	26
Drinking & Waste water	Water Tap, Fountain, Fire Hydrant	Substation, Ambulance Station, Fire Station, Bank, Laboratory, Motorway Junction	11
Digital Infrastructure	Communications Tower, Connection Point	Substation, Water Tower	7
Public Administration	Post Office, Telephone, Townhall, Police	Substation, Water Tower, Wastewater Plant, Connection Point, Bank, ATM, Hospital	31
Food	Barn, Silo, Stable	Water Tower, Wastewater Plant, Fire Station, Police, Connection Point	15
Commercial Facilities	Mall, Department Store, Hotel	Water Tower, Wastewater Plant, Fire Station, Bank, ATM, Communication Points	33
Emergency Services	Police, Fire Station, Ambulance Station	Substation, Water Tower, Wastewater Plant, Hospital, Communication Towers	21
Total			**181**

4.3.1. Step 3a: Define POI category dependencies

The translation from sector-level dependencies to POI-level relationships is achieved by selecting the OpenStreetMap categories that best represent the corresponding facilities in Camerino. For example, the **Health** sector depends on **Energy** for continuous power supply, which at the POI level results in a connection between *Hospitals* and *Power Substations*. Similarly, **Emergency Services** rely on **Digital Infrastructure**, implying that facilities such as the *Red Cross Center* must be associated with an appropriate *Internet Access Point*.

Table 8 summarizes the dependencies identified among POI instances in the Camerino case study, derived from the POI-category relationships described in the companion paper [6].

- **Energy:** Substations depend on communication towers and connection points for real-time monitoring and control of power distribution.
- **Transportation:** Infrastructures such as motorway junctions and aerodromes rely on substations for power, water towers and wastewater plants for utility needs, and communication systems for logistics and traffic management. They are also supported by health and emergency services.
- **Banking:** Banks, ATMs, and payment terminals require stable services from substations, water and wastewater facilities, and communication towers to ensure continuous operations and financial transactions.
- **Health:** Hospitals, clinics, and pharmacies depend on energy, water, waste management systems, and ambulance services. Communication towers support healthcare coordination and emergency response.
- **Water & Wastewater:** Water-related infrastructures (e.g., taps, hydrants) depend on substations, fire and ambulance stations, financial services, and transport hubs to ensure their functionality, especially in emergencies.
- **Digital Infrastructure:** Communication towers and connection points depend on substations and water infrastructure to remain operational and provide connectivity across sectors.
- **Public Administration:** Administrative services like townhalls, post offices, and police stations rely on multiple providers including substations, water systems, digital infrastructure, and health services.
- **Food:** Agricultural and food-related facilities (e.g., barns, silos, stables) depend on utility and emergency services such as water, waste, and fire stations, as well as communication points for supply chain coordination.
- **Commercial Facilities:** Facilities such as malls and hotels depend on energy, water, waste management, fire protection, and banking and communication services for daily operations and consumer services.
- **Emergency Services:** Fire stations, police, and ambulance services rely on power, water, and communication infrastructure, and are further supported by health facilities during emergency interventions.

4.3.2. Step 3b: Define POI instance dependencies

To construct POI-level dependencies for Camerino, we implemented the sectoral relationships by linking POI instances belonging to the corresponding categories. In the absence of detailed infrastructure interconnection data, dependencies were instantiated using

Table 9
List of POIs extracted for the Camerino case study. Node IDs follow the sequential extraction order from the OSM-based dataset and are used consistently throughout the Dependency Risk Graph.

POI sector	POI dependent	POI providers
Public Administration	v_{88}	v_{65}, v_{604}
Drinking & Waste Water	v_{56}	v_{607}, v_{614}
Emergency Services	v_{604}	v_{86}, v_{84}
Health	v_{30}	v_{84}, v_{65}
Banking	v_{18}	v_{84}, v_{65}
Digital Infrastructure	v_{84}	v_{65}, v_{18}
Transport	v_{9}	v_{84}, v_{13}
Commercial Facilities	v_{278}	v_{84}, v_{65}

a geographical proximity criterion, assuming that POIs offering essential services are more likely to interact when located near one another.

Below, we illustrate relevant interconnections within specific sectors, as shown in Table 9.

- **Public Administration**: Governmental facilities (e.g., v_{88}) often depend on emergency service nodes (e.g., v_{604}) and digital or power infrastructure (e.g., v_{65}) to guarantee continuity of operations, especially in crisis situations when decision-making must be fast and well-informed.
- **Drinking & Waste Water**: Critical water infrastructures (e.g., v_{56}) rely on upstream facilities such as pump stations or reservoirs (e.g., v_{607}, v_{614}) to ensure the distribution and treatment of water. These dependencies are essential for sustaining sanitation and public health services.
- **Emergency Services**: Fire stations and emergency responders (e.g., v_{604}) need stable communication channels (e.g., v_{84}) and road access or nearby resources (e.g., v_{86}) to coordinate rapid intervention and manage emergency scenarios efficiently.
- **Health**: Healthcare facilities (e.g., v_{30}) are highly dependent on reliable power infrastructure (e.g., v_{65}) and communication systems (e.g., v_{84}) to support medical equipment, IT networks, and emergency calls, especially during large-scale disasters.
- **Banking**: Financial services (e.g., v_{18}) require robust digital infrastructure (e.g., v_{84}) and uninterrupted electricity supply (e.g., v_{65}) to maintain real-time transactions, ATM operations, and cybersecurity.
- **Digital Infrastructure**: Communication points (e.g., v_{84}) depend on electricity substations (e.g., v_{65}) and in some cases secure facilities (e.g., v_{18}) for housing control systems, illustrating the reciprocal dependencies between critical networks.
- **Transport**: Road segments and transport nodes (e.g., v_{9}) depend on communication infrastructure (e.g., v_{84}) and emergency service facilities (e.g., v_{13}) to ensure operational safety and response capability during traffic incidents.
- **Commercial Facilities**: Essential retail or logistics points (e.g., v_{278}) rely on electrical supply (e.g., v_{65}) and stable communication systems (e.g., v_{84}) to conduct digital transactions and coordinate with suppliers and clients.

4.3.3. Step 3c: Collect failure propagation and recovery action data

This step quantifies the likelihood of failure propagation between POIs and the probability of successful recovery actions, which serve as key inputs for the subsequent risk assessment.

In the absence of empirical interdependency data for Camerino, a categorical probability distribution was adopted to approximate both propagation and recovery dynamics. The same distribution was applied across all sectors, providing a consistent and structured representation of disruption and restoration processes. Failure propagation probabilities reflect the assumption that most disruptions remain localized due to infrastructural redundancies, whereas recovery probabilities capture differences in restoration speed linked to resource availability and operational constraints.

Fig. 3 illustrates the categorical distribution used for both failure and recovery.

4.3.4. Step 3d: Refine failure propagation and recovery action data with local modifiers

After collecting failure-propagation and recovery probabilities for each POI dependency, these values are refined by accounting for local infrastructural and environmental conditions.

Additional POI information provided by the municipality of Camerino was integrated into the OSM dataset, enabling a more detailed representation of local facilities. However, empirical data on failure-propagation and recovery probabilities for these municipal POIs are not available. For this reason, the same simulated probability distributions adopted for OSM-derived POIs were applied uniformly. Although factors such as infrastructure condition, redundancy, and local environmental risks may influence these probabilities, their quantitative effects cannot be estimated in the absence of empirical records.

4.4. Step 4: Create dependency risk graphs for resilience analysis

Using the previously defined dependency structure, the Dependency Risk Graph for Camerino is constructed by assigning impact and recovery parameters to each POI link, enabling time-dependent simulation of cascading effects.

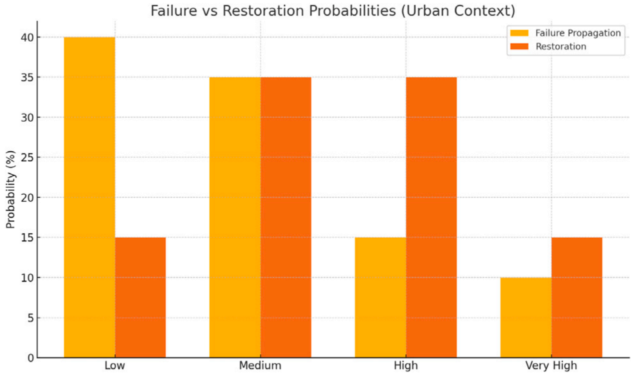

Fig. 3. Step 3c: Categorical probability distribution adopted for failure propagation and recovery in the Camerino case study.

Table 10
Step 4a — probability distributions, parameters, and normalization reference (P_{99}) for maximum social impact and recovery, by sector.

CI sector	Impact distribution	Impact parameters	Recovery parameters	Normalization reference (P_{99})
Energy	Binomial	$n = 900,\ p = 0.15$	$n = 900,\ p = 0.20$	**240**
Transport	Lognormal	$\mu = 850,\ \sigma = 0.13$	$\mu = 850,\ \sigma = 0.18$	**180**
Banking	Binomial	$n = 500,\ p = 0.12$	$n = 550,\ p = 0.14$	**60**
Health	Negative Binomial	$r = 4,\ p = 0.35$	$r = 10,\ p = 0.75$	**90**
Drinking & Waste Water	Binomial	$n = 800,\ p = 0.12$	$n = 800,\ p = 0.15$	**170**
Digital Infrastructure	Poisson	$\lambda = 10$	$\lambda = 12$	**110**
Public Administration	Beta	$a = 2,\ b = 5$	$a = 3,\ b = 6$	**30**
Food	Negative Binomial	$r = 6,\ p = 0.3$	$r = 7,\ p = 0.35$	**85**
Commercial Facilities	Lognormal	$\mu = \ln(100),\ \sigma = 0.8$	$\mu = \ln(120),\ \sigma = 0.9$	**130**
Emergency Services	Poisson	$\lambda = 15$	$\lambda = 20$	**75**

4.4.1. *Step 4a: Collect impact and recovery action metrics data*

In this stage, the key parameters for *impact* and *recovery* are specified for each POI–POI dependency in the Camerino area. Although the MARIS framework supports economic, operational, and social dimensions, the case study focuses solely on the *social impact* domain.

For each dependency, the social impact function is described by three parameters: the maximum number of people affected (I), the time required to reach this maximum (T), and the growth profile (U, where 1 = slow, 2 = linear, 3 = fast). Recovery is represented analogously through parameters $\bar{I}$, $\bar{T}$, and $\bar{U}$.

To ensure consistency across heterogeneous dependencies, all parameters are defined through a structured Likert scale (1–8). The present values serve as illustrative examples, showing how expert knowledge may later be formalized through a standardized elicitation process and integrated via appropriate probability distributions. This approach aligns with established probabilistic frameworks for CI interdependency analysis [10] and social-impact modeling [2].

Maximum Impact & Recovery ($I, \bar{I}$). Sector-specific probability distributions model the maximum number of people affected or recovered (Table 10). Distributions are selected according to sector characteristics: `Binomial` for bounded user populations (e.g., Energy), `Lognormal` for potentially large disruptions (e.g., Transport), `Poisson` for rate-based events (e.g., Digital Infrastructure), and `Negative Binomial` for overdispersed counts (e.g., Health). Recovery distributions follow the same logic but generally reflect faster dynamics or capped capacities. All values are normalized on a 1–8 Likert scale using the 99th percentile (P_{99}) of each distribution.

—

Time of Maximum Impact & Recovery ($T, \bar{T}$). The time required to reach peak impact or recovery is modeled using Lognormal distributions (Table 11), capturing the asymmetric temporal evolution typical of cascading disruptions. Sector-specific parameters reflect expert expectations: longer times for complex systems (e.g., Health, Energy) and shorter cycles for rapidly restored services (e.g., Emergency). Simulated values are discretized into the Likert time scale $\mathcal{T} = \{t_1, \ldots, t_9\}$, ranging from 15 min to 4 weeks.

—

Impact & Recovery Growth ($U, \bar{U}$). Impact and recovery dynamics are categorized as *slow*, *linear*, or *fast*. These profiles capture escalation and restoration behaviors across CI sectors. For example, Public Administration, Health, and Emergency Services show predominantly linear growth, while Digital Infrastructure and Energy tend to exhibit faster escalation. Recovery patterns differ, depending on redundancy, operational readiness, and sector-specific capabilities (Table 12).

Table 11
Step 4a — lognormal parameters and expected durations for impact and recovery time across CI sectors.

CI Sector	Impact time (μ, σ)	Recovery time (μ, σ)	Impact mean duration (min)
Energy	3.3, 0.8	4.1, 0.9	244
Transport	3.2, 0.8	4.2, 1.0	245
Banking	2.3, 0.6	3.0, 0.7	122
Health	3.9, 1.0	4.5, 1.0	229
Drinking & Waste Water	4.3, 0.6	4.2, 0.8	270
Digital Infrastructure	3.9, 0.8	4.1, 0.9	225
Public Administration	4.2, 0.7	4.0, 0.8	260
Food	2.9, 0.8	4.0, 0.9	180
Commercial Facilities	2.5, 0.7	3.5, 0.9	125
Emergency Services	4.1, 0.9	4.0, 1.0	254

Table 12
Step 4a — probabilities of impact and recovery growth profiles across CI sectors.

CI sector	Impact growth (%)	Recovery growth (%)
Public Administration, Health, Emergency Services	30, 40, 30	35, 35, 30
Digital Infrastructure, Drinking & Waste Water, Energy	25, 35, 40	30, 40, 30
Food, Banking, Transport, Commercial Facilities	40, 30, 30	35, 35, 30

Table 13
Step 4b — refined probability distributions for maximum social impact per POI category in camerino, incorporating local context.

POI category	Distribution	Refined key parameters	Characteristic values
Public Administration	Beta	$a = 2,\ b = 5$ (scaled by population and role)	Mean $\approx 0.3 \times$ pop. (adjusted demographically)
Emergency Services	Poisson	$\lambda = 15$ (accounts for terrain and response needs)	Mean = 15 (higher with delayed access)
Health	Negative Binomial	$r = 4,\ p = 0.4$ (based on hospital demand and elderly ratio)	Mean ≈ 6 (driven by vulnerability)
Banking	Poisson	$\lambda = 8$ (limited commercial activity)	Mean = 8 (sensitive to external stressors)
Drinking & Waste Water	Binomial	$n = 700,\ p = 0.1$ (based on households and network resilience)	Mean = 70 (affected by drought/flood risk)
Digital Infrastructure	Lognormal	$\mu = \ln(100),\ \sigma = 0.8$ (captures rare outages)	Mean ≈ 110 (rises with low redundancy)
Transport	Beta	$a = 2,\ b = 3$ (reflects road exposure in hilly terrain)	Mean $\approx 0.4 \times$ range (if key routes affected)
Energy	Binomial	$n = 900,\ p = 0.15$ (based on supply coverage)	Mean = 135 (scales with user demand)
Food	Negative Binomial	$r = 3,\ p = 0.35$ (local supply chain exposure)	Mean ≈ 5 (varies with access and demand)
Commercial Facilities	Lognormal	$\mu = \ln(90),\ \sigma = 0.7$ (variable economic exposure)	Mean ≈ 100 (adjusted for market role)

4.4.2. *Step 4b: Adjust impact and recovery data to the local context*

In this step, the probabilistic assumptions defined in Step 4a are refined by calibrating the distributions for *maximum social impact* (I) and *maximum recovery* ($\bar{I}$) to better reflect Camerino's geographic, demographic, and infrastructural characteristics. This local adjustment increases the realism and robustness of subsequent risk evaluations.

Table 13 reports the final distributions and parameters for each POI category: the third column contains the refined distributional values, while the fourth provides contextualized expected impacts based on local conditions.

The refinement focuses solely on $M_{j,k}$ and $\bar{M}_{j,k}$; temporal ($T_{j,k}$, $\bar{T}_{j,k}$) and growth parameters ($U_{j,k}$, $\bar{U}_{j,k}$) remain unchanged from Step 4a due to the lack of detailed local data to support a robust recalibration.

Camerino's mountainous morphology, limited accessibility, and past seismic events justify higher expected impacts for emergency services, transport, drinking & waste water, and digital infrastructure. A significant elderly population and a large student community increase exposure in public administration and healthcare. Lower expected impacts for banking reflect the city's modest commercial footprint, whereas communication infrastructures are modeled with distributions suited to rare but potentially high-impact failures.

4.4.3. Step 4c: Create dependency risk graphs

For the Camerino application, we construct a single Dependency Risk Graph focused on social impact, denoted as $\hat{G}^s = (V, E, W^s)$. The node set $V = v_k$ contains the 614 POI instances extracted in Step 2, and the edge set $E = e_{jk}$ represents the 114 POI-level dependencies identified in Step 3. The associated weight set W^s includes the failure-propagation and recovery parameters derived from Steps 3c–3d and the impact-recovery characteristics defined in Steps 4a–4b. This graph provides the basis for simulating time-dependent cascading effects across the local infrastructure network.

4.5. Step 5: Evaluate the dependency chain risk

This step evaluates and compares how disruption propagates along the relevant dependency subchains, synthesizing their behavior into resilience metrics to support prioritization of the most vulnerable paths.

4.5.1. Step 5a: Define the dependency chain risk

In this step, the cumulative dependency risk function $\mathbb{D}_{C_i^\ell}(t)$, as defined in Eq. (8), is specified for each subchain C_i^ℓ belonging to the social-specific Dependency Risk Graph $\hat{G}^s$, introduced in Step 4c. This graph focuses exclusively on cascading failures in terms of *social impact*, incorporating both failure propagation and recovery parameters that have been calibrated to reflect the local context of Camerino. The function $\mathbb{D}_{C_i^\ell}(t)$ is computed for each relevant dependency chain identified within $\hat{G}^s$, enabling the evaluation of time-dependent risk levels along interdependent POIs.

4.5.2. Step 5b: Identify relevant subchains in the DRG

Building on the previously introduced *Scenario Failure Set* V_F, in the present case we consider

$$V_F = \{Townhall, Hospital\},$$

where the *Townhall* (v_{145}, Public Administration) constitutes a key administrative hub housed in a seismically vulnerable historical building, and the *Hospital* (v_{30}, Health sector) is critical for emergency response yet potentially compromised by structural damage or accessibility constraints.

The task of this step is to identify the subset of acyclic subchains in the Dependency Risk Graph (DRG) that originate from or intersect with nodes in V_F. These subchains correspond to the *Critical Path Set* here specialized to the case of maximum path length $\ell = 3$. The resulting collection, denoted as $\mathcal{S}_{3,V_F}$, comprises 192 distinct dependency chains.

4.5.3. Step 5c: Evaluate the dependency chain risk

To quantify the time-dependent propagation of disruption along each subchain, the cumulative risk function $\overline{\mathbb{R}}_{\mathcal{S}_{3,V_F}}(t)$ was evaluated through a Monte Carlo framework with $Q = 100$ simulation runs for each subchain $C_i^3 \in \mathcal{S}_{3,V_F}$. In each run, the input parameters were independently sampled from their respective probability distributions, generating an ensemble of realizations

$$\mathbb{D}_{C_i^3}(t) = \{\, \mathbb{D}^{(r)}_{C_i^3}(t) \mid r = 1, \dots, Q \,\}.$$

From this ensemble, the mean cumulative risk at each discrete time step was estimated, yielding a robust representation of the expected disruption trajectory.

To illustrate the heterogeneity of risk propagation patterns, five representative subchains were selected according to three criteria: (i) inclusion of both the most and least resilient chains, (ii) heterogeneity of critical infrastructure subsectors, and (iii) relevance of endpoints in terms of user exposure.

The five selected subchains are:

- **Path 83** (C_{83}^3): *connection point → motorway junction → wastewater plant → town hall*
- **Path 107** (C_{107}^3): *police → hospital → motorway junction → town hall*
- **Path 56** (C_{56}^3): *fire station → hospital → ATM → town hall*
- **Path 12** (C_{12}^3): *substation → wastewater plant → police → town hall*
- **Path 39** (C_{39}^3): *stop position → connection point → fire station → town hall*

The temporal evolution of the mean cumulative risk $\overline{\mathbb{D}}(t)$ for the selected chains is shown in Fig. 4, illustrating how cascading failures propagate across different dependency paths. Risk escalation is strongest in subchains terminating at highly exposed POIs (e.g., hospitals, municipal offices), particularly when these depend on vulnerable upstream nodes such as substations, wastewater plants, or digital communication facilities.

Conversely, chains that include upstream nodes with redundancy or buffering capacity (e.g., police stations, transport hubs, connection points) exhibit a slower and less pronounced increase in $\overline{\mathbb{D}}(t)$, as these elements mitigate or delay disruption propagation.

The non-monotonic, oscillatory patterns observed in some trajectories are not artifacts but arise from the asynchronous interaction between disruption and recovery. As formalized in Eqs. (10)–(11), temporary recoveries may partially offset failures before subsequent cascades occur, producing oscillations consistent with the stochastic dynamics of interdependent infrastructures.

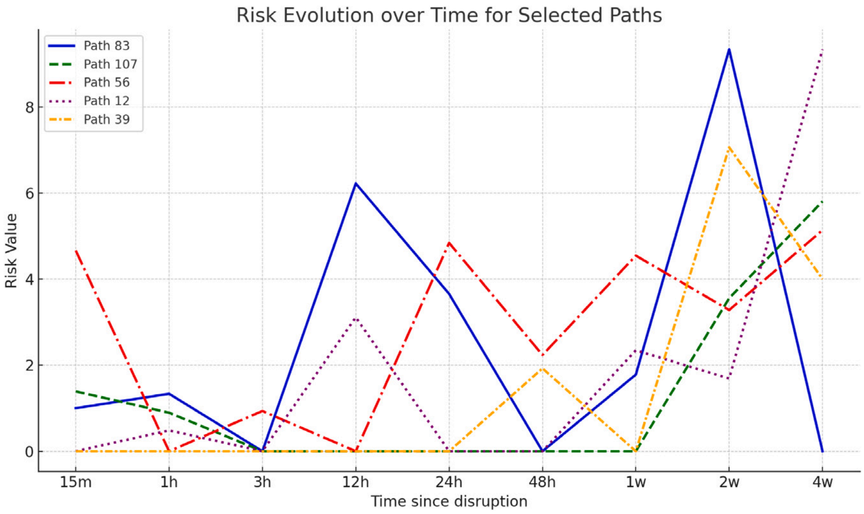

Fig. 4. Temporal evolution according to the Likert scale of the average cumulative risk $\overline{\mathbb{D}}(t)$ for five selected dependency chains.

4.5.4. Step 5d: Compare dependency risk across subchains in the DRG

To enable a synthetic comparison of disruption patterns across the Critical Path Set, the *resilience* value of each subchain was computed from the average cumulative risk over the $Q = 100$ Monte Carlo simulations. The resulting *Resilience Values Set* $\mathbb{R}_{S_{3,V_F}}$ allows direct ranking of subchains based on their ability to limit and recover from cascading failures. High values indicate fast recovery and limited impact, whereas lower values reflect more severe or persistent disruptions.

Among the five representative paths, **Path 83** shows the lowest resilience (82.99%), due to limited redundancy and high user exposure, while **Path 107** achieves the highest score (88.39%) thanks to the stabilizing effect of upstream emergency services. Intermediate profiles (Paths 56 and 12) reflect moderate accumulation, whereas Path 39 exhibits a delayed but sharp escalation linked to transport-originating dependencies.

4.6. Discussion and final remarks

The Camerino case study demonstrated the applicability of the proposed methodology in an urban context highly exposed to seismic hazards. By modeling POI-level interdependencies and simulating disruption-recovery dynamics through a stochastic framework, the analysis revealed notable differences in the vulnerability and resilience of dependency chains.

Subchains terminating at POIs with high user demand, such as the Townhall and the Hospital, showed the steepest increases in cumulative risk. This does not imply the absence of contingency measures, but rather reflects a quantitative amplification effect: facilities serving large user bases naturally elevate cumulative disruption, even when recovery mechanisms are present. These nodes therefore act as amplification points in cascading dynamics. Conversely, paths including nodes with buffering capacity (e.g., police stations, transport hubs, connection points) exhibited slower escalation, mitigating failures before they reached critical user-facing services.

The explicit inclusion of recovery dynamics plays a key role in moderating cumulative risk over time. While high-demand facilities tend to experience sharper increases in risk, recovery functions help limit or reverse this growth, shaping both the timing and the duration of maximum impact. This aspect is particularly relevant for end users, as the framework not only identifies vulnerable dependency chains but also indicates when peak impacts are likely to occur — information that can support preparedness and targeted mitigation planning.

The Camerino application serves primarily as a proof of concept to demonstrate the operational applicability and scalability of MARIS, rather than as empirical validation against past events. Direct comparison with real disruptions, such as the 2016 earthquake, is limited by the availability of open data and confidentiality constraints on critical infrastructure information. Validation activities are planned within the Horizon Europe *MULTICLIMACT* project, including workshops with local authorities and operators to compare simulated cascading and recovery dynamics with observed data and expert insight.

Beyond its methodological contributions, the framework has clear policy relevance. By quantifying cascading and recovery dynamics, MARIS supports implementation of the CER Directive and the Sendai Framework, enabling authorities to identify critical dependency chains, prioritize preventive measures, and design short-term recovery actions based on quantitative evidence. At municipal and regional scales, the approach can inform resilience indicators, investment priorities, and civil-protection planning, helping coordinate multiple stakeholders and align local practices with EU-wide resilience goals.

Although applied here to seismic risk, the MARIS framework is flexible and can be extended to other hazards – including floods, heat waves, and energy disruptions – making it a versatile tool for emergency preparedness and resilience planning across diverse territorial contexts.

5. Conclusions

This work presented an extension of the MARIS methodology as an open-data-based framework for assessing cascading failure risk in interdependent critical infrastructure systems. By explicitly modeling POI-level dependencies and integrating disruption and recovery dynamics, the framework enables a time-sensitive evaluation of systemic vulnerabilities and supports the estimation of resilience across social, economic, and operational dimensions.

The Camerino case study, developed within the Horizon Europe *MULTICLIMACT* project, demonstrated the ability of the methodology to capture differences in the resilience of dependency chains. Subchains terminating at high-demand facilities amplified cumulative impacts due to the large number of users involved, whereas chains including nodes with buffering capacity showed more gradual escalation. The explicit inclusion of recovery dynamics allowed not only the assessment of disruption magnitude but also the identification of the timing of peak impacts, providing actionable insights for preparedness and mitigation.

It should be stressed that the data employed were designed to be realistic but are not strictly representative of Camerino's actual infrastructure. Results should therefore not be interpreted as an evaluation of the city's current recovery capacity, but as a demonstration of the framework's potential.

Future developments will focus on enhancing the operational relevance of MARIS through the integration of real-time and multi-hazard data. Achieving credible results, however, requires continuous collaboration with local stakeholders, so that dependency structures and recovery parameters are grounded in real-world conditions and validated in practice.

CRediT authorship contribution statement

Antonio Di Pietro: Writing – original draft, Software, Methodology, Formal analysis, Conceptualization. **Alberto Tofani:** Writing – review & editing. **Clemente Fuggini:** Writing – review & editing. **Celina Solari:** Writing – original draft. **Gabriele Oliva:** Writing – review & editing.

Disclaimer

The risk assessments and results presented in this publication are derived from simulations and models developed for research purposes within the MULTICLIMACT project. They do not constitute official evaluations, nor should they be considered as a stand-alone basis for emergency planning, infrastructure interventions, or public policy decisions. Where applicable, data have been anonymized or generalized to avoid the identification of specific assets or sensitive locations.

Declaration of competing interest

The authors declare the following financial interests/personal relationships which may be considered as potential competing interests: Antonio Di Pietro reports financial support was provided by Horizon Europe. If there are other authors, they declare that they have no known competing financial interests or personal relationships that could have appeared to influence the work reported in this paper.

Acknowledgments

The authors acknowledge the European Union for funding the MULTICLIMACT project (Grant Agreement No. 101123538). They also thank the Municipality of Camerino for supporting the identification of model-relevant Points of Interest (POIs) based on open-source resources (e.g., OpenStreetMap).

Data availability

Data will be made available on request.

References

[1] A. Fekete, J. Estrany, M.Á.A. Ramírez, Cascading impact chains and recovery challenges of the 2024 Valencia catastrophic floods, Discover Sustainability 6 (2025) 586, http://dx.doi.org/10.1007/s43621-025-01483-4.

[2] Rae Zimmerman, Carlos E. Restrepo, Analyzing cascading effects within infrastructure sectors for consequence reduction, Nat. Hazards Rev. 17 (1) (2017) 04015005, http://dx.doi.org/10.1061/(ASCE)NH.1527-6996.0000193.

[3] UNISDR, Terminology on disaster risk reduction, 2017, United Nations Office for Disaster Risk Reduction (UNDRR), URL https://www.undrr.org/terminology/resilience.

[4] United Nations Office for Disaster Risk Reduction, Sendai framework for disaster risk reduction 2015–2030, 2015, Adopted at the Third UN World Conference on Disaster Risk Reduction, Sendai, Japan, URL https://www.undrr.org/publication/sendai-framework-disaster-risk-reduction-2015-2030.

[5] European Union, Directive (EU) 2022/2557 of the European parliament and of the Council on the resilience of critical entities, 2022, Official Journal of the European Union, L333, 27.12.2022, URL https://eur-lex.europa.eu/legal-content/EN/TXT/?uri=CELEX%3A32022L2557.

[6] Antonio Di Pietro, Francesco Cavedon, Giorgos Stergiopoulos, Vittorio Rosato, Modeling fault dynamics of interdependent assets in complex urban environments using open-data: Extended version, SN Comput. Sci. 6 (6) (2025) 564, http://dx.doi.org/10.1007/s42979-025-04037-7.

[7] V. Rosato, A. Di Pietro, P. Kotzanikolaou, G. Stergiopoulos, G. Smedile, Integrating resilience in time-based dependency analysis: A large-scale case study for urban critical infrastructures, in: V. Rosato, A. Di Pietro (Eds.), Issues on Risk Analysis for Critical Infrastructure Protection, IntechOpen, Rijeka, 2021, http://dx.doi.org/10.5772/intechopen.99358.
[8] George Stergiopoulos, Panayiotis Kotzanikolaou, Marianthi Theocharidou, Dimitris Gritzalis, Risk mitigation strategies for critical infrastructures based on graph centrality analysis, Int. J. Crit. Infrastruct. Prot. 10 (2015) 34–44.
[9] Steven M. Rinaldi, James P. Peerenboom, Terrence K. Kelly, Identifying, understanding, and analyzing critical infrastructure interdependencies, IEEE Control Syst. Mag. 21 (6) (2001) 11–25, http://dx.doi.org/10.1109/37.969131.
[10] Min Ouyang, Review on modeling and simulation of interdependent critical infrastructure systems, Reliab. Eng. Syst. Saf. 121 (2014) 43–60, http://dx.doi.org/10.1016/j.ress.2013.06.040.
[11] R. Pant, K. Barker, C.W. Zobel, Static and dynamic metrics of resilience for interdependent infrastructure systems, Reliab. Eng. Syst. Saf. 125 (2015) 92–102, http://dx.doi.org/10.1016/j.ress.2014.01.016.
[12] Yuan Gong, Kai Sun, Qian Duan, Temporal modelling of cascading failures and recovery processes in interdependent infrastructure networks, Reliab. Eng. Syst. Saf. 223 (2022) 108504.
[13] Ling Yan, Kai Xie, Peng Li, Dynamic resilience analysis of interdependent infrastructure systems using multi-layer networks, Saf. Sci. 142 (2021) 105395.
[14] Hao Zheng, Wenhao Li, Yi Ding, A Monte Carlo simulation framework for assessing cascading failures in multi-sector critical infrastructures, Int. J. Crit. Infrastruct. Prot. 41 (2023) 100590.
[15] Zhen Wang, Ren Xu, Yong Bian, A probabilistic multi-layer network model for assessing interdependencies among critical infrastructures, Saf. Sci. 168 (2024) 106478.
[16] T. Yabe, et al., Behavior-based dependency network framework for assessing economic resilience, Nat. Commun. (2024).
[17] A. Wróbel, Efficiency and susceptibility in critical infrastructure networks, Int. J. Crit. Infrastruct. Prot. (2022).
[18] Y. Almoghathawi, et al., Identification of critical nodes in interdependent infrastructure systems, Reliab. Eng. Syst. Saf. (2021).
[19] M. Theoharidou, et al., Risk-based criticality analysis for interdependent infrastructures, Int. J. Crit. Infrastruct. Prot. (2009).
[20] G. Stergiopoulos, P. Kotzanikolaou, D. Gritzalis, Using centrality metrics in dependency risk graphs, Int. J. Crit. Infrastruct. Prot. (2015).
[21] Y. Shi, et al., Dynamic repair strategies for cascading failures in complex networks, IEEE Trans. Netw. Sci. Eng. (2024).
[22] U. Mbanaso, et al., Modeling Nth-order dependencies in critical infrastructure with neural networks, J. Infrastruct. Syst. (2020).
[23] M. Akbarzadeh, et al., Multi-order dependency quantification in cyber-physical systems, IEEE Trans. Syst. Man Cybern. (2019).
[24] Y. Zhang, et al., Infrastructure vulnerability detection using visual saliency and tone mapping, J. Infrastruct. Syst. (2020).
[25] H. Liu, et al., Machine learning approaches for resilience assessment in high-consequence systems, Reliab. Eng. Syst. Saf. (2023).
[26] Alexander Fekete, Common criteria for the assessment of critical infrastructures, Int. J. Disaster Risk Sci. 2 (2011) 15–24, http://dx.doi.org/10.1007/s13753-011-0002-y.
[27] A. Tofani, G. D'Agostino, A. Di Pietro, S. Giovinazzi, M. Pollino, V. Rosato, S. Alessandroni, Operational resilience metrics for complex inter-dependent electrical networks, Appl. Sci. 11 (13) (2021) 5842, http://dx.doi.org/10.3390/app11135842.
[28] The White House, Presidential policy directive 21 (PPD-21) on critical infrastructure security and resilience, 2013, https://obamawhitehouse.archives.gov/the-press-office/2013/02/12/presidential-policy-directive-critical-infrastructure-security-resil. (Accessed 21 July 2025).
[29] European Union Agency for Cybersecurity (ENISA), Interdependencies of Critical Infrastructures: European Perspective, Technical report, ENISA, Heraklion, Greece, 2020, URL https://www.enisa.europa.eu/publications/interdependencies-of-critical-infrastructures. (Accessed 21 July 2025).
[30] William E. Vesely, Fred F. Goldberg, Nancy H. Roberts, Donald F. Haasl, Fault Tree Handbook, in: NUREG-0492, U.S. Nuclear Regulatory Commission, Washington, DC, 1981, URL https://www.nrc.gov/docs/ML1007/ML100780465.pdf.
[31] Roy Billinton, Ronald N. Allan, Reliability Evaluation of Engineering Systems: Concepts and Techniques, second ed., Springer, Boston, MA, 1992, http://dx.doi.org/10.1007/978-1-4899-0685-0.
[32] Susan L. Cutter, Bryan J. Boruff, W. Lynn Shirley, Social vulnerability to environmental hazards, Soc. Sci. Q. 84 (2) (2008) 242–261, http://dx.doi.org/10.1111/1540-6237.8402002.
[33] Reinhard Diestel, Graph Theory, fifth ed., Springer, Berlin, Heidelberg, ISBN: 978-3-662-53621-6, 2017, http://dx.doi.org/10.1007/978-3-662-53622-3.